

Analysis of discontinuities in quantum waveguide structures

A. Weisshaar, J. Lary, S. M. Goodnick, and V. K. Tripathi

Department of Electrical and Computer Engineering, Oregon State University, Corvallis, Oregon 97331

(Received 31 July 1989; accepted for publication 11 September 1989)

We have used the modal expansion of the wave function in the discontinuity region based on the superposition principle together with a mode-matching technique to investigate the transmission characteristics of semiconductor quantum wire structures with discontinuities. Our calculations compare quite well with published results for the theoretical transmission coefficient and experimental conductance of a T-stub and split-gate geometry, respectively. We apply this technique to analyze the effect of right-angle bends in narrow quantum wires which show strong resonant behavior due to the presence of discontinuities in this geometry.

Recent experimental results on split-gate field-effect transistors,^{1,2} in which conduction plateaus as a function of gate voltage were observed, demonstrate that the behavior of electrons in nanometer structure devices is similar to the behavior of electromagnetic waves in guided wave structures. Such quantum waveguide behavior is evident for structures with dimensions less than the mean free path of the electrons so that motion is essentially ballistic except for the scattering associated with the discontinuities. Phase coherent electronic effects have been previously observed in other structures such as resonant tunneling diodes³ and the observation of Aharonov-Bohm oscillations in metallic⁴ and semiconductor⁵ rings. The possibility of utilizing quantum coherent effects in semiconductor structures for active devices has been suggested by several authors.^{6,7} In particular, Sols *et al.*⁷ have proposed a transistor based on modulation of the transmission coefficient in a T-stub configuration which is predicted to have a large transconductance for single-mode operation.

In this letter we describe an accurate and computationally efficient method for analyzing a wide range of transitions and discontinuities in quantum waveguide structures. Here we have applied this technique to the T-stub configuration discussed above and pinched wire configurations which resemble the geometry of the split-gate transistor experiments. Our method is based on a mode-matching technique which was proposed by Kühn⁸ to compute the electromagnetic fields in waveguide circuits with discontinuities and has been extended to calculate the transmission characteristics of microstrip discontinuities.^{9,10} We assume that the particles inside the quantum waveguide are governed by the time-independent Schrödinger wave equation in the effective mass approximation with the boundary condition $\psi = 0$ at the edges of the structure (hard wall approximation). We define our coordinate system such that z corresponds to the propagation axis of the waveguides with uniform cross section so that the solution of the time-independent Schrödinger equation is separable and has the general form

$$\psi = (Ae^{\gamma z} + Be^{-\gamma z})\phi_{n,m}(x,y), \quad (1)$$

where $\gamma = ik_z$ is the propagation constant (k_z being the z component of the wave vector), while n and m correspond to the mode or subband indices associated with bound-state solutions in the x and y directions.

To demonstrate our method we calculate the transmis-

sion probability for a T-stub configuration as given by Sols *et al.*⁷ (see inset of Fig. 1). Here the discontinuity in the wire structure is only in the x direction so that the solution may be assumed to be independent of the y coordinate without any loss of generality. For analyzing the T-stub configuration, we define four regions as shown in the inset of Fig. 1. The application of the mode-matching technique requires a complete set of modes with orthogonal properties in all four regions. With the general solution for a quantum waveguide in the form of Eq. (1), a complete set of modes in regions I and II is readily found as

$$\psi^I = \sum_{m=1}^{\infty} (a_m^I e^{\gamma_m^I z} + b_m^I e^{-\gamma_m^I z}) \sin\left(\frac{m\pi}{w_1} x\right), \quad (2a)$$

$$\psi^{II} = \sum_{m=1}^{\infty} (a_m^{II} e^{-\gamma_m^{II}(z-w_2)} + b_m^{II} e^{\gamma_m^{II}(z-w_2)}) \sin\left(\frac{m\pi}{w_1} x\right), \quad (2b)$$

where m is the mode number (subband index), $\gamma_m^I = \gamma_m^{II} = ik_{z,m}^I$ are the propagation constants, and a_m^I , b_m^I and a_m^{II} , b_m^{II} are the wave amplitudes for reference planes at $z = 0$ and $z = w_2$, respectively. Region III is terminated by a hard wall at $x = w_1 + L$. Thus a complete set of modes in region III is given by

$$\psi^{III} = \sum_{m=1}^{\infty} c_m \sinh[\gamma_m^{III}(x - w_1 - L)] \sin\left(\frac{m\pi}{w_2} z\right), \quad (3)$$

with propagation constant $\gamma_m^{III} = ik_{x,m}^{III}$ and amplitude c_m of the standing waves for the reference plane at $x = w_1$. A form

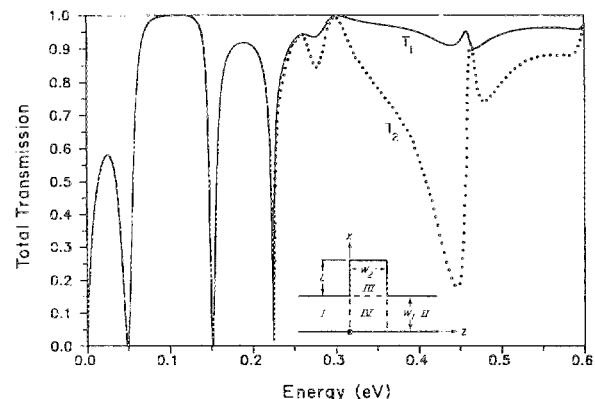


FIG. 1. Total transmission probabilities from mode 1 (T_1) and mode 2 (T_2) as a function of electron energy ($w_1 = w_2 = L = 10$ nm).

of the solution in region IV which is suitable for the application of the mode-matching technique can be constructed by alternately placing a hard wall ($\psi = 0$) at the boundaries between regions I and IV ($z = 0$), II and IV ($z = w_2$), and III and IV ($x = w_1$), and then superimposing the solutions

$$\begin{aligned} \psi^{IV} = & \sum_{m=1}^{\infty} \left[d_m^a \sinh(\gamma_m^I z) \sin\left(\frac{m\pi}{w_1} x\right) \right. \\ & + d_m^b \sinh[\gamma_m^I (z - w_2)] \sin\left(\frac{m\pi}{w_1} x\right) \\ & \left. + d_m^c \sinh(\gamma_m^{III} x) \sin\left(\frac{m\pi}{w_2} z\right) \right]. \end{aligned} \quad (4)$$

Applying the boundary conditions for ψ and its derivative at the interface in the same manner as in Ref. 8 leads to an infinite set of linear equations which interrelates the wave amplitudes of regions I and II. For numerical solutions this infinite set of equations is truncated to M equations where M is the highest order mode to be considered in order to achieve a desired convergence or accuracy.

From the requirement of flux conservation, the total transmission probability from mode n in region I to all modes in region II is given as

$$T_n = \sum_m b_m^{II} b_m^{II*} (\gamma_m^{II} - \gamma_m^{II*}) / a_n^I a_n^{I*} (\gamma_n^I - \gamma_n^{I*}). \quad (5)$$

The total transmission probability from the lowest mode ($n = 1$) and from the second lowest mode ($n = 2$) in region I to region II for a T-stub with various widths w_1 , w_2 and stub lengths L has been computed and fast convergence with an increasing number of modes has been found. The results for a symmetrical T-stub configuration with $w_1 = w_2 = L = 10$ nm as a function of electron energy which is referenced to the bottom of the lowest subband are shown in Fig. 1. The curves are virtually identical to those shown by Sols *et al.*⁷ for the same structure using a tight-binding Green's function technique.

A further application of our method is in the analysis of a constriction or pinched wire structure, for which conduction oscillations have been observed.^{1,2} The conductance G of the pinched wire due to the constriction of width w_p (inset of Fig. 2) in the limit of zero temperature has been given by Fisher and Lee¹¹ from a linear response theory:

$$G = \frac{e^2}{h} \sum_n T_n(E_f), \quad (6)$$

which also corresponds to the Landauer form¹² in the limit of large reflection in the wider region. In Eq. (6) the summation is over all propagating modes at the input, and $T_n(E_f)$ is the total transmission probability from mode n at the input to the output at the Fermi energy E_f . The conductance, given in units of e^2/h , is shown in Fig. 2 for different lengths L_{\min} of the constriction and different one-dimensional (1-D) electron densities. It is assumed that the size of the constriction is varied by means of a gate voltage and the resulting depletion region has the same extensions in longitudinal and transversal directions as indicated in the inset of Fig. 2. Thus, the theoretical conductance gives the qualitative behavior observed experimentally.^{1,2} Note that for $L/w_p \gtrsim 1$, the constriction becomes long enough to damp out the

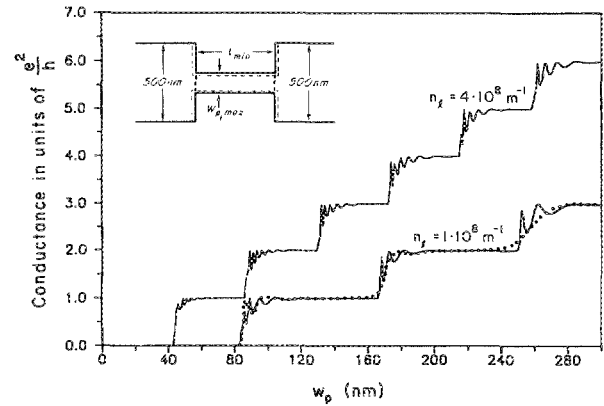


FIG. 2. Conductance for a pinched wire configuration as a function of pinching width w_p for two different 1-D electron densities n_1 . The length L of the pinched region increases by the same amount by which the pinching width w_p is decreased. Solid lines correspond to $L_{\min} = 450$ nm; dotted line corresponds to $L_{\min} = 75$ nm. In all cases $T = 0$ K.

evanescent modes in the pinched region and thus the conductance shows a resonant structure. Such structure was observed by Szafer and Stone¹³ who used a recursive Green's function technique as well as a direct matching scheme. For $L/w_p \lesssim 1$ the tunneling of electrons through the constriction cannot be neglected. Hence, a resonant structure in the conductance is not visible and the steps become less sharp which, again, is in agreement with Szafer and Stone.¹³

It should be noted that the above two structures can also be analyzed by using a direct matching technique at the two interfaces associated with the step discontinuities in the waveguide. However, for larger stub lengths of the T structure, the method presented here leads to faster convergence and reliable accurate results. In addition, the significant feature of our method is that it is a general technique which can be applied to transitions and discontinuities where direct mode matching is not feasible as demonstrated by the following case of a right-angle bend in the quantum waveguide.

We now consider a single right-angle bend and divide it into three regions as shown in the inset of Fig. 3 (top bend). A complete set of modes in regions I and II can be found in

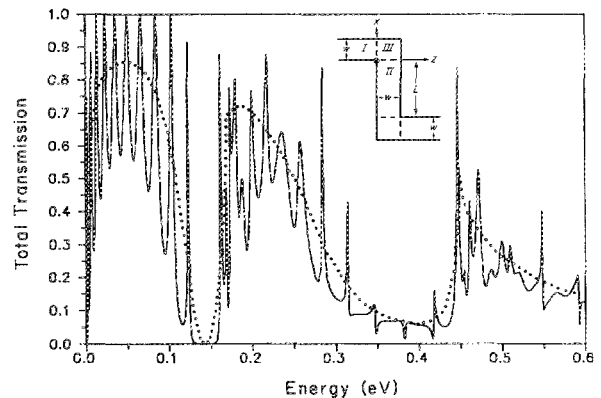


FIG. 3. Total transmission probability from mode 1 (T_1) as a function of electron energy ($w = 10$ nm, $L = 60$ nm). The dotted curve shows the transmission probability T_1 for a single right-angle bend; the solid line shows T_1 for the double bend configuration.

the same manner as the solution in region I for the T-stub configuration. The solution in region II is of the same form as that in region I with interchanged coordinates x and z . To find a complete set of modes with orthogonal properties in region III, we alternately place a hard wall ($\psi = 0$) at the boundary between regions I and III ($z = 0$) and II and III ($x = 0$) and then superimpose the solutions. We have computed the total transmission probability from the lowest mode in region I ($n = 1$) to region II for right-angle bends with various widths w . The dotted line in Fig. 3 shows the result for a bend with width $w = 10$ nm as a function of electron energy which is referenced to the bottom of the lowest subband in region I. The right-angle bend shows strong resonant behavior as a function of energy with total reflection of the incident electrons with energies of ~ 0.14 eV. For bends with arbitrary width w the results are identical to Fig. 3 (dotted line) with appropriate scaling of the energy axis by $(w_1/w)^2$, where w_1 corresponds to the width w used in Fig. 3 ($w = 10$ nm).

By cascading two single right-angle bends, separated by length L , we obtain the configuration of a double bend as shown in the inset of Fig. 3. The total transmission probability from the lowest input mode to the output is computed for a width $w = 10$ nm and length $L = 60$ nm as shown in Fig. 3 (solid line). The double bend shows additional resonances superimposed on the resonances of the single right-angle bend. These fine structure resonances are due to the cavity of length L which arises when cascading two single bends, and they move closer together and become sharper as the length L is increased.

In summary, we have presented a method well suited to the analysis of discontinuities such as transitions and bends in quantum wire structures. Our calculated results for the T-stub configuration are virtually identical to those published

by Sois *et al.*⁷ using a much different technique. Our results for the pinched wire give the qualitative behavior of the conductance which was observed experimentally for similar structures^{1,2} and show good agreement with published theoretical calculations. The method we propose in this letter is a general one and can be applied to study a variety of geometries including multiport configurations. This accurate and computationally efficient method has been implemented on IBM AT's and compatible desktop computers and thus does not require supercomputer resources.

The research was partially supported under the U. S. Office of Naval Research contract No. N00014-89-J-1894. One of the authors (JL) acknowledges the support of IBM, Essex Junction, Vermont.

¹B. J. van Wees, H. van Houten, C. W. J. Beenakker, J. G. Williamson, L. P. Kouwenhoven, D. van der Marel, and C. T. Foxon, *Phys. Rev. Lett.* **60**, 848 (1988).

²D. A. Wharam, T. J. Thornton, R. Newbury, M. Pepper, H. Ahmed, J. E. F. Frost, D. G. Hasko, D. C. Peacock, D. A. Ritchie, and G. A. C. Jones, *J. Phys. C* **21**, L209 (1988).

³T. C. L. Solner, W. D. Goodhue, P. E. Tannenwald, C. D. Parker, and D. D. Peck, *Appl. Phys. Lett.* **43**, 588 (1983).

⁴R. A. Webb, S. Washburn, C. P. Umbach, and R. B. Laibowitz, *Phys. Rev. Lett.* **54**, 2696 (1985).

⁵S. Datta, M. R. Melloch, S. Bandyopadhyay, R. Noren, M. Vaziri, M. Miller, and R. Reifenberger, *Phys. Rev. Lett.* **55**, 2344 (1985).

⁶S. Datta, *Superlatt. Microstruct.* **6**, 83 (1989).

⁷F. Sols, M. Macucci, U. Ravaioli, and K. Hess, *Appl. Phys. Lett.* **54**, 350 (1989).

⁸E. Kühn, *Arch. Elek. Übertragung* **27**, 511 (1973).

⁹W. Menzel and I. Wolff, *IEEE Trans. Microwave Theory Tech.* **MTT-25**, 107 (1977).

¹⁰A. Weisshaar and V.K. Tripathi, *Electron. Lett.* **25**, 1138 (1989).

¹¹D. S. Fisher and P. A. Lee, *Phys. Rev. B* **23**, 6851 (1981).

¹²R. Landauer, *Philos. Mag.* **21**, 863 (1970).

¹³A. Szafer and A.D. Stone, *Phys. Rev. Lett.* **62**, 300 (1989).